

Multi-Length Scale Characterization of the Gibeon Meteorite using Electron Backscatter Diffraction

Matthew M. Nowell and John O. Carpenter

EDAX-TSL, Draper UT
matt.nowell@ametec.com

The Gibeon meteorite is a differentiated iron meteorite that fell in Namibia, Africa in prehistoric times, with fragments spread over an area 70 miles wide and 230 miles long. The Gibeon fall was initially discovered in 1836, and hundreds of thousands of kilograms of fragments have been recovered. These fragments represent the iron core of a meteorite that cooled and crystallized over thousands of years (Norton 2002).

The microstructure of the Gibeon meteorite, which is primarily an iron-nickel alloy, consists of two phases: kamacite, a body-centered cubic material and taenite, a face-centered cubic material that metallurgists would refer to as ferrite and austenite respectively. This material initially crystallizes as taenite, and as the temperature decreases, transforms into kamacite. This meteorite is classified as a Fine Octahedrite (Of) with an average Nickel content of approximately 7.9%

Electron Backscatter Diffraction (EBSD) is a Scanning Electron Microscopy (SEM) based characterization technique that is commonly used to analyze crystalline materials in both material and earth sciences. This technique has been used successfully to examine many different meteorites, including the Gibeon meteorite, and to investigate the mechanisms of the formation of the different phases present (Nolze and Geist 2004, Goldstein and Michael 2006, He *et al.* 2006, Hutchinson and Hagström 2006). The goal of this work was to use EBSD to examine the Gibeon meteorite on a characterization length-scale of centimeters to nanometers.

A sample of the Gibeon meteorite measuring approximately 19mm x 16mm was prepared for EBSD analysis by first mounting the sample in a conductive thermocompressive mounting medium and then mechanically polishing the surface down to a 0.3 μ m alumina suspension finish. The final polish stage used 0.05 μ m colloidal silica on a vibratory polisher for approximately 4 hours. The details of the polishing procedure have been previously published (Nowell *et al.* 2005). After polishing, the sample was removed from the mount to better facilitate imaging and EBSD data collection over the entire sample area. Because of the high specimen tilt values used during EBSD work (75° in this case), careful selection of the analysis area, specimen size, and SEM working distance helps to minimize the collision hazard between the sample and the pole piece. During polishing, extra care was taken to try and obtain and maintain parallel surfaces between the polished and non-polished sides of the specimen.

The EBSD data was collected using an FEI XL-30 FEG SEM operating at 20kV acceleration voltage and an approximate incident beam current of 3.75nA. An EDAX Hikari EBSD detector operating with OIM

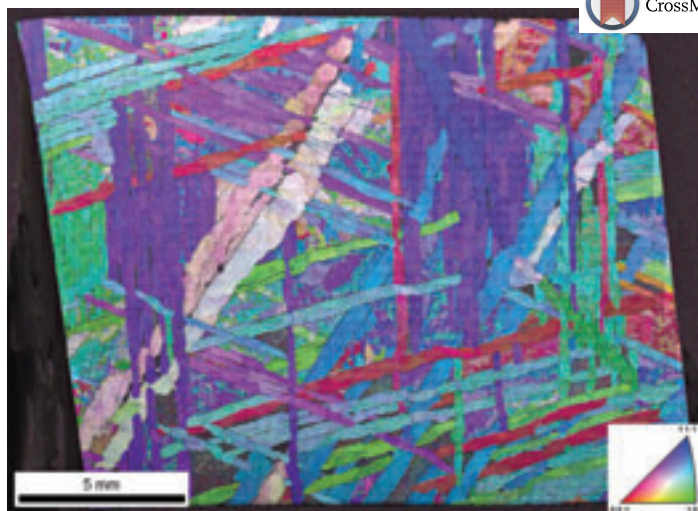


Figure 1 – Orientation map of Gibeon meteorite sample collected with combination beam-stage scanning. The stereographic triangle is colored to represent crystal directions aligned with the sample normal direction. This key is used with all subsequent orientation maps.

Data Collection software V5.2 was used at speeds of 200 indexed points per second. For EBSD mapping, EBSD patterns are collected and analyzed from a grid of periodically positioned measurement points. From each pattern, the crystallographic orientation, phase (from a list of candidate phases) and pattern quality are determined. Correlations between adjacent measurements can also be used to determine grain

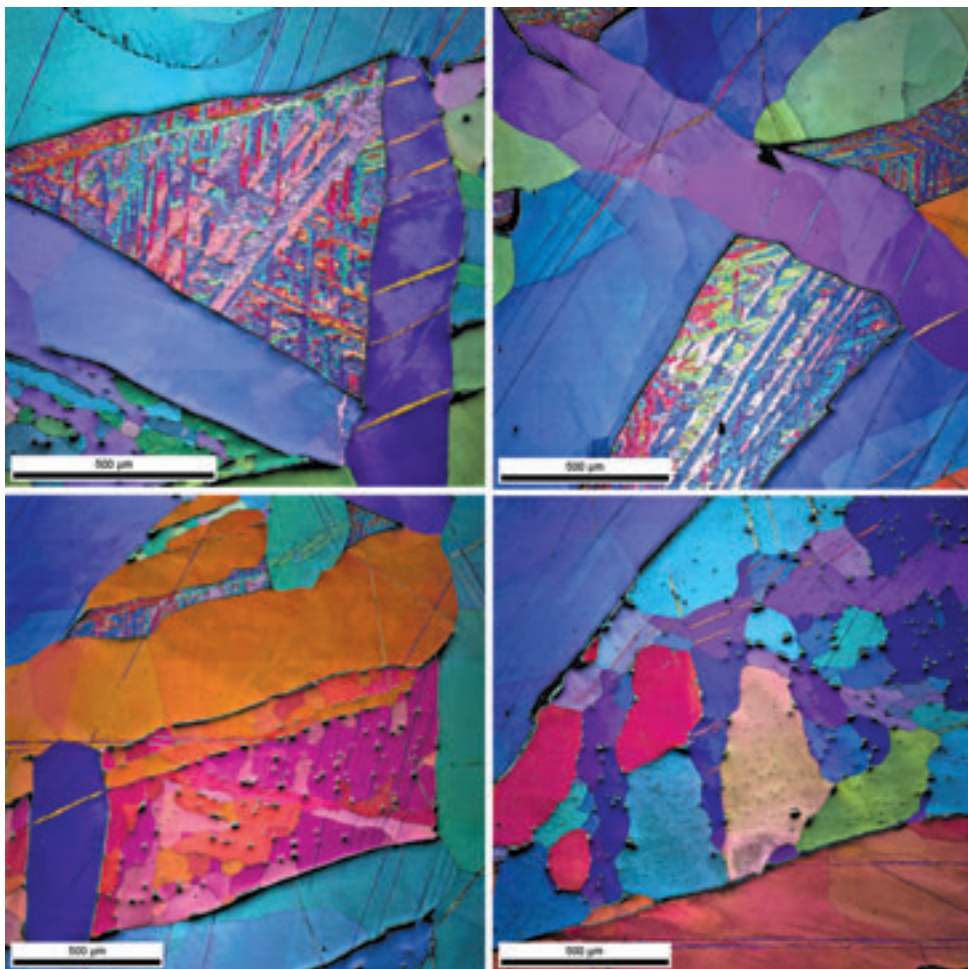


Figure 2 – Orientation maps collected at a-top left) 150X magnification – 650nm step size, b-top right) 125X magnification – 800nm step size, c-bottom left) 110X magnification – 850nm step size, and d-bottom right) 125X magnification – 1,000nm step size of coarse and fine plessite regions.

Let 4pi take you beyond the capability of any SEM/STEM on the market with

RevolutionEDX

X-ray Microanalysis Systems optimized for productivity & ease of use

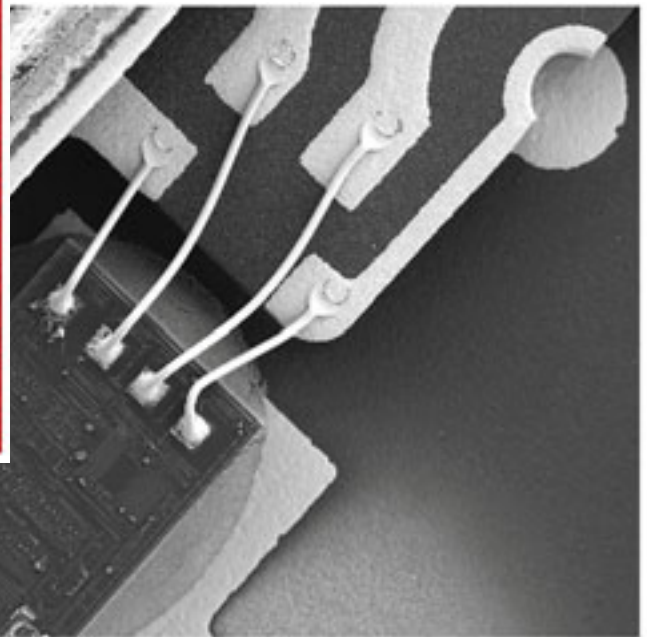
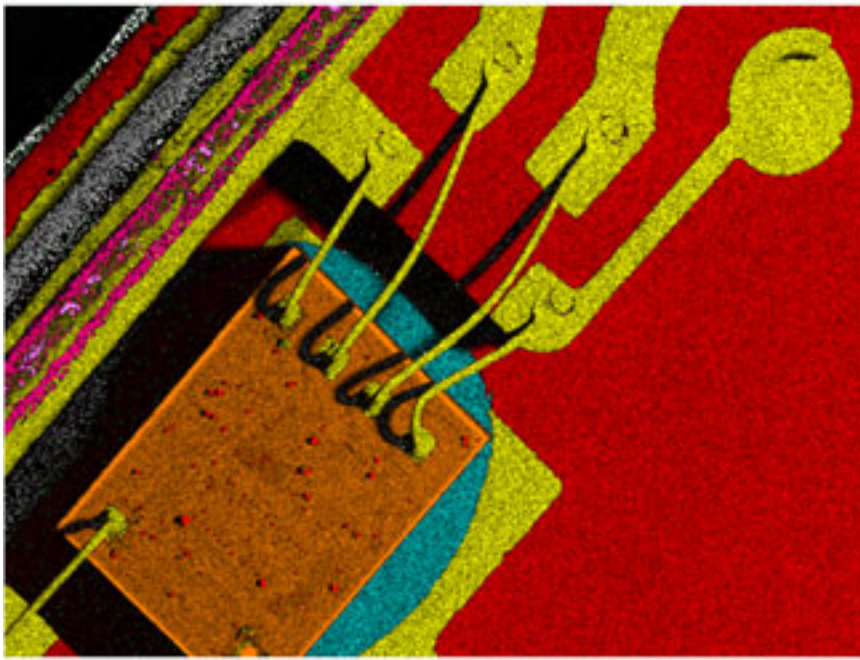
- Silicon-drift technology detectors
 - Liquid Nitrogen-free
 - High-throughput
 - 10 or 30 mm² sensor
- Work over a network via Gigabit Ethernet
- Easy to use: one-click acquisition for spectra, images, maps, spot probes and line scans
- **Dynamic Dwell Modulation™** – spend maximum time on areas of interest while continuing to obtain x-ray data from the entire area
- Robust auto peak-ID based on real-time full deconvolution of acquired x-ray spectra



High resolution: 129eV or better
Super-ultra-fast spectrum imaging

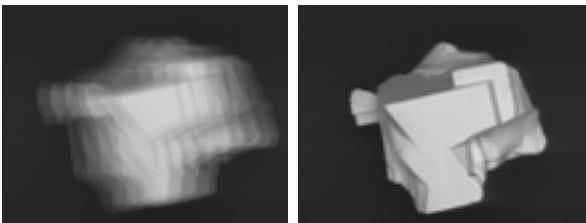
*Unique features save time
& production costs*

Event-Streamed Spectrum Imaging™
Collect x-ray spectrum images at electron imaging speeds



Spatial Frame Lock™

Real-time electron-beam drift correction



Available TODAY only from



www.4pi.com • sales@4pi.com
4pi Analysis, Inc. 919.489.1757

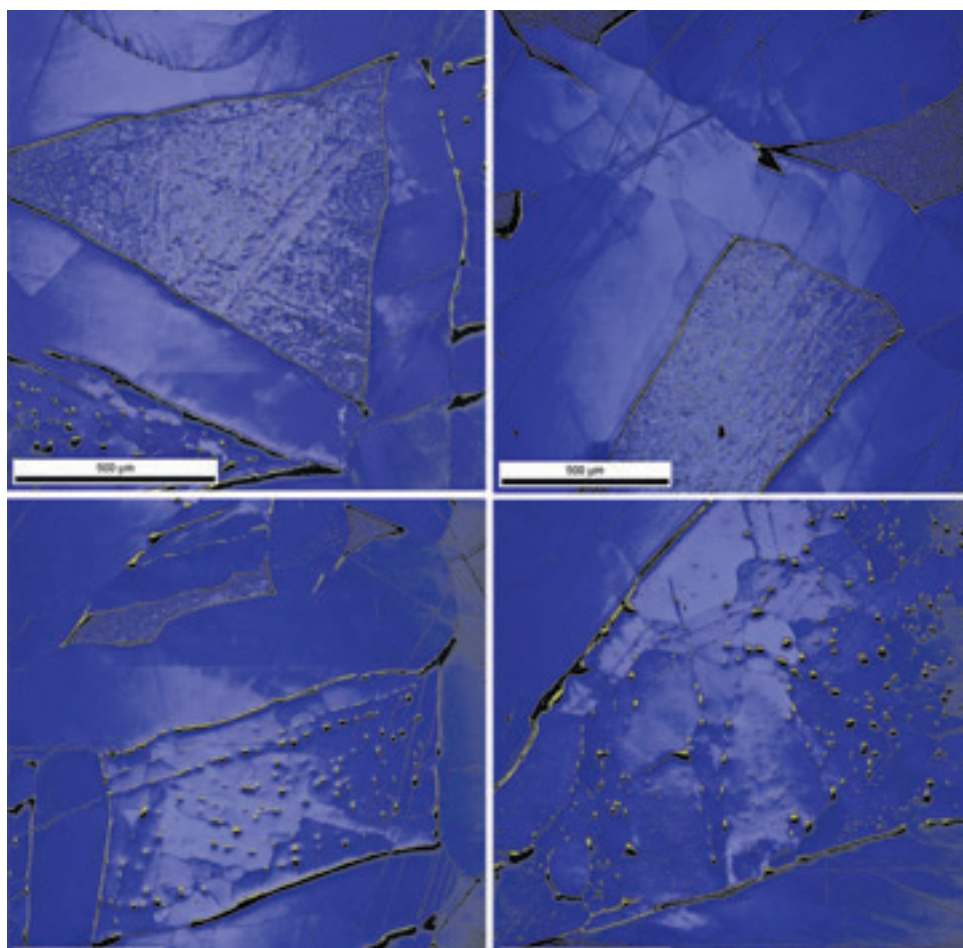


Figure 3 – Phase maps with kamacite colored blue and taenite colored yellow collected at a-top left) 150X magnification – 650nm step size, b-top right) 125X magnification – 800nm step size, c-bottom left) 110X magnification – 850nm step size, and d-bottom right) 125X magnification – 1,000nm step size of coarse and fine plessite regions.

size, grain shape, and grain boundary misorientations.

A macrostructure was visible to the naked eye after preparation. Traditionally EBSD mapping is obtained through using either beam scanning or stage movement, with beam scanning being the most common. With beam scanning, the electron beam is positioned at each measurement location by applying a discrete voltage to the SEM scanning coils. This method requires a dynamic adjustment of the EBSD pattern center location for accurate orientation determination as the position of the electron beam/specimen interaction point relative to the EBSD detector phosphor screen changes for each measurement location. The maximum analysis area is limited by the lowest possible magnification for a given SEM working distance. However this is often impractical as defocusing of the beam occurs as it is positioned along the tilted surface. Instead it is recommended that a dynamic focus correction, which keeps the beam focused across the tilted surface, be used. Using this correction can limit the lowest available magnification. Even with this correction, some scanning artifacts can occur. A trapezium distortion caused by the beam scanning of a highly tilted surface is always present, but typically more noticeable at lower magnifications (Nolze 2007). A rhomboidal distortion can also occur if the sample surface plane is not accurately aligned and

parallel to the stage. It is because of this that care is taken during the sample preparation stage to maintain a parallel sample surface. There is also a limited precision in the voltage applied to the scanning coils. This typically manifests itself when using small spacings between measurements at low magnifications. As an estimate, this problem occurs when the step size between measurements is 1,000X smaller than the width of the analysis area. Small variations in the applied voltages result in oscillations of the beam position. This results in more diffuse EBSD patterns at low magnifications than those that could be obtained at higher magnifications. This is also a function of the grain size of the material of interest. In spite of these limitations, beam scanning is the most commonly used method because of the inherent acquisition speed benefits. It is possible to position the electron beam and capture and analyze an EBSD patterns at speeds greater than 300 points per second. However beam scanning could not be used to characterize the entire sample, as only a fraction was observable at the lowest possible magnification.

In comparison, stage scanning is much slower due to the time required to physically position the stage between measurements. With stage scanning the beam is fixed at a position in space and the stage is used to translate the specimen so that the measurements are obtained from the specified grid positions. Ideally, all EBSD mapping would utilize stage scanning, as stage scanning can eliminate trapezium distortion, and minimize rhomboidal distortion by using

three axis stage control (X/Y/Z) to keep the sample surface in the analysis plane. However, typical stage positioning times are orders of magnitude slower than beam scanning (approximately 2 seconds per point on the XL-30) which can make large (in terms of number of data points) scans impractical. There is also a limit to the precision with which the stage can be positioned that effectively limits the minimum step size. Of course, it is also necessary to have a stage that can be controlled remotely.

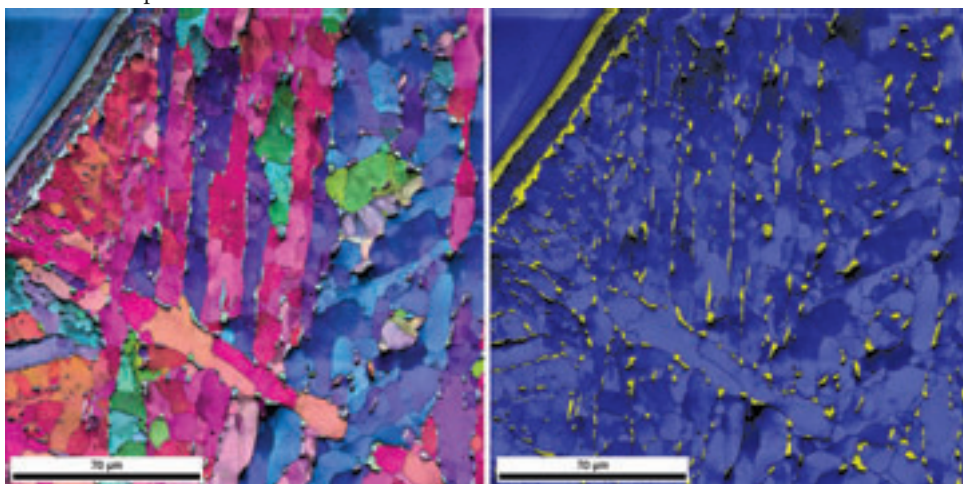


Figure 4a-left) Orientation and b-right) Phase maps of fine plessite region at 1,000X magnification – 100nm step size.

11

MEGAPIXELS

High Definition Digital TEM Cameras

AMT's HOT NEW LINE

**TEM
INTEGRATION**

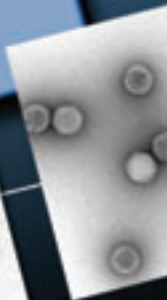
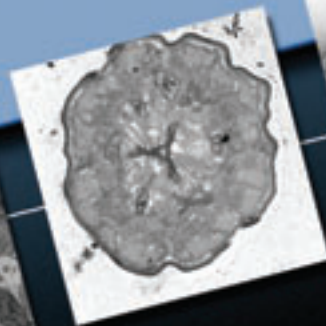
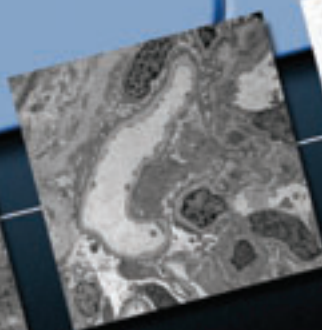
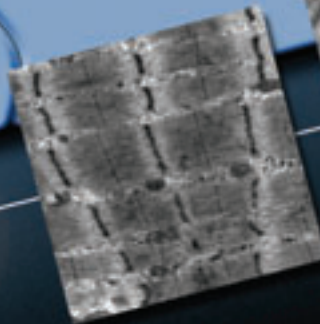
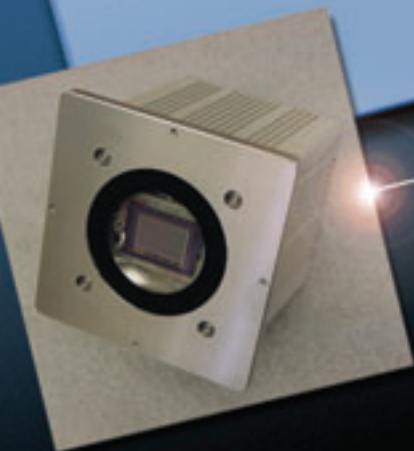
**FASTEST
DISPLAY**

**LARGEST FIELD
OF VIEW**

**SIDE MOUNT
& BOTTOM MOUNT**

**BUILT-IN
RELIABILITY**

**PROVEN
SUPPORT**



Advanced Microscopy Techniques Corporation

3 Electronics Avenue • Danvers, MA 01923

978-774-5550 • www.amtimaging.com

To analyze the entire area of the Gibeon meteorite sample, a hybrid solution using a combination of beam and stage scanning was used. Beam mapping was used at a 500X magnification to analyze a 360 μm x 360 μm area with an 8 μm step size between grid measurements. Stage translation was then used to reposition the analysis region at an adjacent area and beam mapping used again. This process was repeated to cover the entire 20.9mm x 15.3mm area of interest, which resulted in an analyzed area consisting of 59 horizontal regions and 43 vertical regions for a total of 2,537 regions of interest. The data from these regions were then automatically combined together to create a montage of the entire field of view. This data collection method provides a compromise that utilizes the speed of beam scanning while facilitating the large analysis areas available through stage scanning. In this example, only 2,537 stage movements were required, while nearly 5,000,000 data points were collected. Data collection time per field was approximately 12 seconds for EBSD capture and analysis, and 2

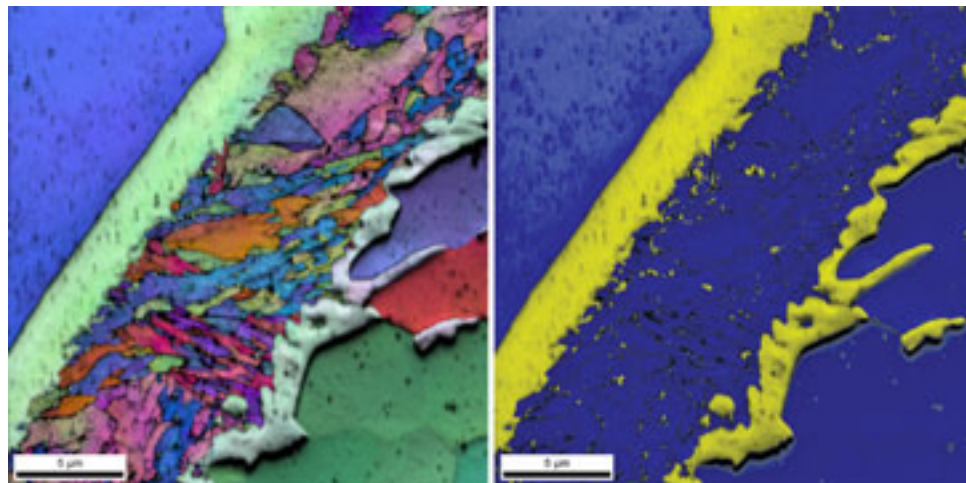


Figure 5a-left) Orientation and b-right) Phase maps of plessite transition region at 8,000X magnification - 25nm step size.

seconds for stage translation. The 500X magnification was selected to minimize trapezium distortion. Lower magnifications are typically not recommended as the resulting distortions can cause artifacts in the data montaging. Using a tilt-corrected field of view for each frame is also recommended. The selected step size of 8 μm is also larger than the expected precision limits of the automated stage. If this were not the case, positioning errors would also be more noticeable.

Results from the combination beam-stage mapping are shown in Figure 1. Here an orientation map shows the crystal orientation relative to the surface normal direction. The orientation map is combined with an EBSD image quality map to enhance microstructural contrast, and this convention is used in all maps presented. Bands of kamacite are present in a Widmanstätten structure. Interestingly, according to Norton, this structure was previously discovered and published by William Thompson in 1804, 4 years prior to an oral communication by Count Widmanstätten, and this structure could more fairly be called the Thompson structure. More interestingly, further insult is often added by sometimes attributing this prior discovery to a different William Thompson, also known as Lord Kelvin, who wasn't born until 1824. This structure evolves from the slow cooling (approximately 1°C per 1,000 years (Narayan and Goldstein 1985)) of an initial single crystal of taenite. The spatial arrangement of the kamacite bands are related to crystallographic orientation of the prior taenite phase. The bands are aligned in only one of four directions, which correspond to the traces of the {111} planes of the prior taenite crystal. These bands are between 200 μm and 500 μm wide and several millimeters long. Intermixed within the Widmanstätten structure are regions of plessite, which is a dual phase mixture of kamacite and taenite. However with the 8 μm step size used, it is difficult to fully resolve the microstructure

within the plessite regions.

Additional scans at magnifications between 110X and 150X were collected at different plessite regions with smaller step sizes (between 650nm to 1,000nm). Figures 2a-2d show the orientations maps from these scans, and figures 3a-3d show the phase maps depicting the spatial distribution of the kamacite and taenite. These images show plessite regions with differing spatial scales of microstructure. Within the coarse plessite, the taenite phase is clearly defined and mostly located adjacent to kamacite grain boundaries. The kamacite grains are hundreds of microns in equivalent diameter. At this magnification, the fine plessite appears as a fractal-like structure mirroring the Widmanstätten structure seen within the complete sample scan. This observation is repeated and highlighted in figures 4a-4b, where images from a fine plessite region collected at 1,000X magnification and step size of 100nm are shown. Again taenite, albeit on a finer scale, is present at the kamacite grain boundaries. Both the coarse and fine plessite are bordered by taenite. Hutchinson and Hagström suggest that these plessite regions are formed by a combination of displacive and diffusional transformations and that the microstructural size differences could be attributed to the variance of nucleation sites available during cooling (Hutchinson 2006).

The transition region between the Widmanstätten kamacite and a fine plessite region was examined at 8,000X magnification and 25nm step size, and the results shown in figures 5a-5b. The transition region consists of two parallel layers of taenite sandwiching a region of fine-grained kamacite. The layer adjacent the kamacite has a smoother interface while the layer adjacent the plessite is much more irregular. This can also be seen in less detail in figures 4a-4b. Within

the fine-grained kamacite, smaller grains of retained taenite, some smaller than 80nm, were also observed.

The characterization of the Gibeon meteorite using EBSD provides insight into the formation, transformation, and distribution of the kamacite and taenite phases. In addition to providing information on the thermal history of the meteorite, the characterization methods used and microstructural information obtained can also be applied to similar phenomena and issues present in modern steel research such as measuring retained austenite and understanding transformation induced plasticity. The combination of high spatial resolution and the ability to analyze large areas through stage and combination beam-stage scanning makes EBSD a useful tool for characterizing a wide range of materials. ■

References

- Goldstein, J.I. and Michael, J.R. (2006), *Meteoritics and Planetary Science* **41** (4) 553-570.
- He, Y., Godet, S., and Jonas, J. (2006) *Journal of Applied Crystallography* **39** 72-81.
- Hutchinson, B. and Hagström, J. (2006) *Metallurgical and Materials Transactions A* **37A** (6) 1811-1818.
- Narayan, C. and Goldstein, J.I. (1985) *Geochim. Cosmochim. Acta.* **49** 397-410.
- Nolze, G. (2007), *Ultramicroscopy* **107** (2-3) 172-183.
- Nolze, G. and Geist, V. (2004), *Crystal Research and Technology* **39**(4) 343-352.
- Norton, O.R. (2002), *The Cambridge Encyclopedia of Meteorites*. Cambridge University Press, Cambridge, U.K.
- Nowell, M.M., Witt, R.A., and True, B.W. (2005) *Microscopy Today* **13** (4) 44-48

The new **2007-2010 EMS CATALOG** is now available!



Your one-stop shop for the latest products and solutions for Microscopy and Histology!

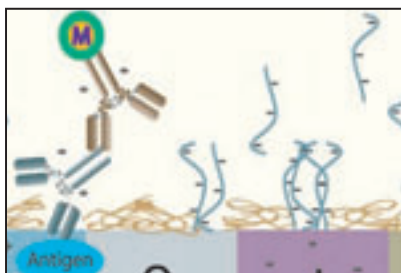
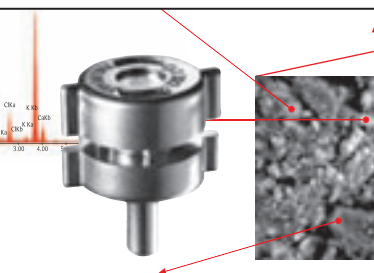
Exacting Research demands only the Highest Quality Products.

Introducing the 2007–2010 EMS Catalog, your comprehensive source for chemicals, supplies, accessories, and equipment for Microscopy, Histology and all fields of biological and materials research.

Featuring new and revolutionary products, including:

- C-flat™ Holey Carbon Grids for cryo-TEM
- Ilford Photography Papers and Photochemicals
- WETSEM™ Capsules for Hydrated SEM Samples
- DuraSIN™ Substrates for TEM & X-ray
- Diatome Oscillating Diamond Knife
- PathScan Enabler III
- Ultra-Thin Carbon Tabs
- Plunge Freezer
- EMS 9000 Precision Pulsed Laboratory Microwave Oven
- State-of-the-Art Oscillating Tissue Slicers
- NioProbe and TipCheck for AFM
- Aurion ImmunoGold Reagents and Accessories
- EMS LYNX Tissue Processor
- MAG*¹*CAL®
- EMS Carbon Coaters and Sputter Coaters

Application Notes • More Technical Support • Enhanced Product Lines • Revolutionary Products



QuantomiX WETSEM™ • AURION Newsletters™ • Diatome Diamond Knives • C-flat™ Holey Carbon Grids

To request our new catalog, please call or write us today,
or visit us online at www.emsdiasum.com

**Electron
Microscopy
Sciences**

P.O. Box 550 • 1560 Industry Rd. • Hatfield, Pa 19440
(215) 412-8400 • Toll Free: 1-(800) 523-5874
Fax: (215) 412-8450 or 8452
email: sgkock@aol.com • stacie@ems-secure.com
www.emsdiasum.com